



Gastric cancer risk-scoring system based on analysis of a competing endogenous RNA network

Min Liu^{1#}, Jing Li^{2#}, Zhengkai Huang³, Yuejun Li^{4,5}

¹Department of Respiratory Medicine, The Affiliated Hospital of Hunan Academy of Chinese Medicine, Changsha 41006, China; ²Department of Oncology, The First Hospital of Hunan University of Chinese Medicine, Changsha 410007, China; ³College of Integrated Chinese Medicine and Western Medicine, Hunan University of Chinese Medicine, Changsha 410208, China; ⁴Department of Oncology, The Third Affiliated Hospital of Hunan University of Chinese Medicine, Zhuzhou 412000, China; ⁵Department of Oncology, The First Affiliated Hospital of Hunan College of Chinese Medicine, Zhuzhou 412000, China

Contributions: (I) Conception and design: Y Li; (II) Administrative support: Y Li; (III) Provision of study materials or patients: Z Huang; (IV) Collection and assembly of data: J Li, Z Huang; (V) Data analysis and interpretation: M Liu, J Li; (VI) Manuscript writing: All authors; (VII) Final approval of manuscript: All authors.

[#]These authors contributed equally to this work.

Correspondence to: Yuejun Li. Department of Oncology, The Third Affiliated Hospital of Hunan University of Chinese Medicine, Zhuzhou 412000, China; Department of Oncology, The First Affiliated Hospital of Hunan College of Chinese Medicine, Zhuzhou 412000, China.
Email: liyuejun97@foxmail.com.

Background: Long noncoding RNAs (lncRNAs) can play vital roles in tumor initiation, progression, invasion, and metastasis. However, the functional role of the lncRNA-based competing endogenous RNA (ceRNA) networks in gastric cancer (GC) is still unclear. We aimed to identify novel lncRNAs and their association with GC prognosis.

Methods: The lncRNA, miRNA, and mRNA expression profiles of GC patients data were obtained from The Cancer Genome Atlas (TCGA) database. Differentially expressed genes (DEGs) were identified using the edge-R package. Then, the relationship among lncRNAs-miRNAs-mRNAs was integrated into a constructed ceRNA network with Cytoscape software. Using Cox regression analysis, a risk score system based on DEGs associated with patient prognosis in GC was established. Finally, a nomogram was founded to predict the prognosis of GC patients.

Results: A total of 971 differentially expressed lncRNAs (DElncRNAs), 144 differentially expressed miRNAs (DEmiRNAs) and 2,789 differentially expressed mRNAs (DEmRNAs) were identified and found to be associated with GC risk. Using the bioinformatics method, a ceRNA network involving 62 DElncRNAs, 21 DEmiRNAs and 59 DEmRNAs was constructed. Based on the results of the Cox regression analysis, a risk-scoring system involving 3 lncRNAs (i.e., ADAMTS9-AS1, C15orf54, and AL391152.1) was set up for the survival analysis of GC patients. The area under the receiver operating characteristic (ROC) curve for the risk-scoring system was 0.674, with a C-index of 0.64 [95% confidence interval (CI): 0.59–0.69, P=2.806485e–08]. Univariate and multivariate Cox regression analyses demonstrated that the risk-scoring system was an independent prognostic factor for GC. The risk-scoring system is positively associated with advanced tumor grade. The expression of these 3 lncRNAs were validated in GEPIA database. A nomogram based on these 3 lncRNAs was created to predict the prognosis of GC patients.

Conclusions: Our study established a novel lncRNA-expression-based ceRNA network and an ADAMTS9-AS1-C15orf54-AL391152.1-based risk-scoring system, which can be used to predict the prognosis of GC patients.

Keywords: Competing endogenous RNA (ceRNA); gastric cancer (GC); long noncoding RNA (lncRNA)

Submitted Dec 26, 2019. Accepted for publication Apr 17, 2020.

doi: 10.21037/tcr-19-2977

View this article at: <http://dx.doi.org/10.21037/tcr-19-2977>

Introduction

Gastric cancer (GC) is the third leading cause of cancer-related mortality, accounting for approximately 783,000 deaths (1 in every 12 deaths) globally in 2018 (1). To date, gastrectomy and chemotherapy are still the main therapeutic options for patients with GC (2). Many new agents, such as pembrolizumab, avelumab and rilotumumab, have been investigated in patients with GC but didn't demonstrate efficacy (3,4). Due to its high prevalence, low survival, and limited treatment choices, GC remains an important clinical practice challenge.

Recently, a number of studies aimed to find molecular biomarkers to prognosticate survival or select appropriate therapeutic strategies for patients with GC. However, most of the studies failed in the validation studies (5). Therefore, the establishment of potential biomarkers and therapeutic targets as well as individualized approaches for treatment is urgently required (3,6).

Long noncoding RNAs (lncRNA) are a group RNAs with a length of at least 200 nucleotides that do not encode proteins. lncRNAs have been recognized to possibly play pivotal biological roles in tumor initiation, progression, invasion, and metastasis (7-9). Salmena *et al.* hypothesized about the existence of a complex competing endogenous RNA (ceRNA) network (10). Numerous studies have confirmed that lncRNAs can regulate messenger RNA (mRNA) transcription by acting as microRNA (miRNA) sponges to suppress the function of miRNA (11-15). For instance, TTTY15 lncRNA can promote the progression of prostate cancer via miRNA let-7 sponging, thus increasing the expression of CDK6 and FN1 (13). FAM225A sponges miR-510-3p/miR-1275 and upregulates ITGB3 to promote nasopharyngeal carcinoma tumorigenesis and metastasis (15). HAGLR lncRNA regulates metastasis and epithelial-mesenchymal transition in esophageal cancer by acting as a microRNA-143-5p sponge to bind lysosome-associated membrane glycoprotein 3 (LAMP3) (14).

The present study aimed to screen out novel lncRNAs for prognosis of patients with GC and to provide new insights into the potential features of lncRNAs as therapeutic targets. Toward this goal, we constructed a lncRNA-based prognostic risk-scoring system based on the ceRNA network. A prognostic nomogram including lncRNA expression and clinical information was established to evaluate the survival rate probability, which can facilitate for clinical use. Our analysis used The Cancer Genome Atlas (TCGA) data of GC patients.

Methods

Data retrieval and analysis

The lncRNA, miRNA and mRNA expression profiles as well as clinical data of GC patients were retrieved from the TCGA database (<http://tcga-data.nci.nih.gov/tcga/>). TCGA database contains multiplatform molecular profiles along with clinicopathological information of various cancer types (16). A total of 410 GC tissues and 42 adjacent normal tissues were subjected to miRNA analysis, while 343 GC patients and 30 normal controls were included for lncRNA and mRNA analysis. The present study was carried out in accordance with the guidelines published by TCGA (http://cancergenome.nih.gov/publications/publication_guidelines). Thus, it was not necessary to obtain further ethical approval.

Identification of differentially expressed lncRNAs, miRNAs and mRNAs in GC

Differentially expressed lncRNAs, miRNAs, and mRNAs were defined and encoded using the Ensembl database (<http://www.ensembl.org/index.html>). The differentially expressed genes (DEGs) were obtained using the "edge-R" package in R software. lncRNA with an absolute log₂-fold change >2 and P values <0.01 was regarded as differentially expressed lncRNA (DELncRNA), whereas miRNA and mRNA with an absolute log₂-fold change >1.5 and adjusted P values <0.05 were regarded as differentially expressed miRNA (DEmiRNA) and differentially expressed mRNA (DEmRNA), respectively. The gplots and heatmap packages in R were adopted to generate volcano plots and heat maps for the DEGs.

ceRNA network construction

The interaction pairs between DELncRNAs and DEmiRNAs were predicted using the miRcode database (17). The StarBase v2.0 database (<http://starbase.sysu.edu.cn/>) was used to modify the miRNA sequences (18). The interaction pairs between DEmiRNA and DEmRNAs were retrieved using the miRDB, miRTarBase, and TargetScan databases (19-21). Only those mRNAs that were represented in all 3 databases were selected as target mRNAs; these were further intersected with the identified DEmRNAs to determine potential DEmiRNA-targeted DEmRNA. Finally, the ceRNA network was established

based on the interaction pairs of DEmiRNA-DEmRNA and DElncRNA-DEmiRNA, and was visualized using Cytoscape version 3.7.2 software (<http://www.cytoscape.org/>) (22).

Establishment of a protein-protein interaction (PPI) network

We aimed to clarify the interactions among DEmRNAs involved in ceRNA network. To do this, we constructed a PPI network. DEmRNAs were imported into the STRING database (<http://string-db.org/>), the search model was chosen as “multiple proteins”, the species was set as “Homo sapiens,” and a score >0.4 was set as the minimum interaction threshold.

To obtain the barplot figure and hub-genes, the downloaded string-interactions.tsv file was imported into R to generate the barplot figure.

Functional and signaling pathway enrichment analysis

To reveal the potential biological process and signaling pathway of DEmRNAs associated with the ceRNA network, Gene Ontology (GO) functional enrichment analysis and Kyoto Encyclopedia of Genes and Genomes (KEGG) pathway enrichment analyses were performed using “clusterProfiler” package in R software. The threshold values were set as: $P < 0.01$ and the false discovery rate (FDR) < 0.05 .

Identification of prognostic signatures for GC

To assess the prognostic values of the identified DEGs, survival analyses were carried out using the “survival” package in R software. Survival curves were produced by using Kaplan-Meier estimates, and were compared statistically using the log-rank test. Univariate Cox analysis was employed to identify significant relationships ($P < 0.001$) between overall survival (OS) and each DEG expressed in the ceRNA network. Subsequently, multivariate Cox regression analysis was applied to explore the role of DEGs in GC, by calculating the risk scores as the sum of the production of each gene and its coefficient [hazard ratio (HR)]. According to the median risk score, GC patients were categorized into 2 cohorts: the high-risk group and the low-risk group. The survival distributions of these two groups were compared using the log-rank test. The effects

of the DEGs (high-risk group versus low-risk group) on OS were determined using the area under the receiver operating characteristic (ROC) curve, namely, AUC under a binomial proportion confidence interval (CI), which was determined with the “survival ROC” package in R, to explore the sensitivity and specificity for predicting GC survival. A scatter plot and interactive distribution-based scatter plot for assessing the performance of the prognostic model were created.

Independence assessment for prognostic system based on risk-scorings

To assess the independent predictive power of prognostic system based on risk-scorings, univariate and multivariate Cox regression analyses were carried out to evaluate the effects of the risk-scoring system along with other clinical variables of GC patients on OS risk-scorings. The results are shown using forest_plots, which were generated with the “survival” package in R. lncRNAs involved in the risk-scoring were validated using Gene Expression Profiling Interactive Analysis (GEPIA) (<http://gepia.cancerpku.cn/index.htm>) (23).

Association analyses between the risk-scoring system and clinicopathological features

In order to explore the associations between the risk-scoring system and clinicopathological characteristics, we performed the chi-square test was conducted via “beeswarm” package in R. Age at diagnosis, gender, TNM stage, and tumor grade were included into analyses.

Gene set enrichment analysis (GSEA)

GSEA were performed to identify enriched KEGG pathways to disclose the potential biological mechanisms of the risk-scoring system. Statistical significance was set as $P < 0.05$ and FDR < 0.25 .

Construction the prognostic nomogram

Based on the results of the multivariate Cox regression analyses of the independent assessment, a prognostic nomogram for OS was generated with the “rms” package in R. Calibration plots were generated to calculate the predictive performance of the prognostic nomogram.

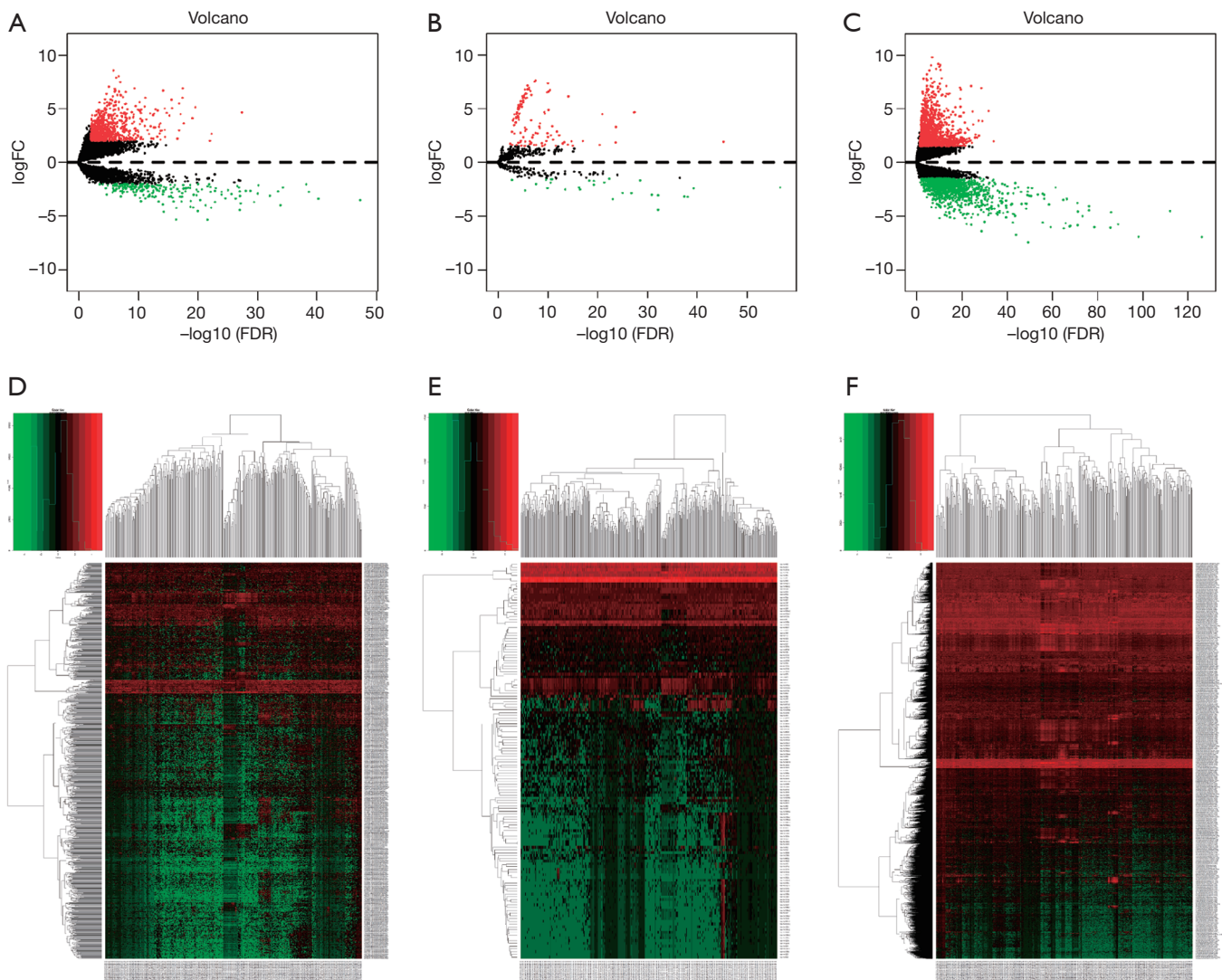


Figure 1 Identification of gastric cancer-associated DEGs. Volcano maps of the DElncRNAs (A), DEMiRNAs (B) and DEMRNAs (C). Heatmaps of the DElncRNAs (D), DEMiRNAs (E) and DEMRNAs (F) associated with risk of GC. DEG, differentially expressed genes; DElncRNAs, differentially expressed lncRNAs; DEMiRNAs, differentially expressed miRNAs; DEMRNAs, differentially expressed mRNAs; GC, gastric cancer.

Results

Differential expression of lncRNAs, miRNAs and mRNA in GC patients

Differential expression analysis revealed that 971 (206 downregulated and 765 upregulated, see at <http://fp.amegroups.cn/cms/2a3ae55f8fbf64907670c1ed3e3d3bb7/tcr-19-2977-1.pdf>, <http://fp.amegroups.cn/cms/0efcd47ff7014a67b5df1aa55a46c98a/tcr-19-2977-2.pdf>) DElncRNA, 2,789 (1,282 downregulated and 1,508

upregulated, see at <http://fp.amegroups.cn/cms/0363dc616251418fc6b7f4219bc63890/tcr-19-2977-3.pdf>, <http://fp.amegroups.cn/cms/c0d33e14c33a482164410347f6eeac8c/tcr-19-2977-4.pdf>) DEMRNAs, and 144 (27 downregulated and 117 upregulated, see at <http://fp.amegroups.cn/cms/8d352a4fb17ce56cb7cd921f1d87e8cf/tcr-19-2977-5.pdf>, <http://fp.amegroups.cn/cms/6b73711adf7879be43569be7a7faabc4/tcr-19-2977-6.pdf>) DEMiRNAs were associated with GC. The distributions of all DEGs in $-\log(\text{FDR})$ and logFC dimensions are presented in the

Table 1 Representative relationships between lncRNAs and miRNAs in gastric cancer

lncRNA	miRNA
IGF2-AS	hsa-mir-519d, hsa-mir-122
C15orf54	hsa-mir-301b, hsa-mir-372, hsa-mir-373, hsa-mir-143, hsa-mir-195, hsa-mir-182
AL357153.1	hsa-mir-301b, hsa-mir-183, hsa-mir-217, hsa-mir-383
AP002478.1	hsa-mir-551a, hsa-mir-372, hsa-mir-373, hsa-mir-195, hsa-mir-519d, hsa-mir-182, hsa-mir-184, hsa-mir-205, hsa-mir-508, hsa-mir-122
LINC00221	hsa-mir-301b, hsa-mir-372, hsa-mir-373, hsa-mir-96, hsa-mir-143, hsa-mir-519d, hsa-mir-182, hsa-mir-204, hsa-mir-21, hsa-mir-217, hsa-mir-508

Table 2 Representative relationships between miRNAs and mRNAs in gastric cancer

miRNA	mRNA
Has-mir-519d	HMGB3, SMOC, CFL2, PGM2L1, FAM129A, E2F1, SOX4, CYBRD1, NETO2, ATAD2, POLQ, SLC16A9
hsa-mir-182	ULBP2, HOXA9, TCEAL7, FOXF2, CITED2, PRKAA2, NPTX1
hsa-mir-145	SERPINE1, MEST, ANGPT2
hsa-mir-204	HCAR2, IL11, NPTX1, HOXC8, FOXC1, CHRDL1
hsa-mir-373	LEFTY1, CADM2, PBK, ATAD2, CFL2, TMEM100

form of volcano maps (*Figure 1A,B,C*). The numerical data representing the expression profiles of DEGs are shown in the form of heatmaps (*Figure 1D,E,F*).

ceRNA network of GC patients

The ceRNA network was constructed as follows. First, 62 DElncRNAs, 21 DEmiRNAs, and 315 pairs of lncRNA and miRNA interaction were screened using the miRcode dataset and the Perl program (*Table 1*). Then, the 21 miRNA-targeted mRNAs were selected from the miRTarBase, miRDB, and TargetScan databases. The DEGs represented in all 3 databases were ultimately chosen, and those not involved in DE mRNAs were discarded (*Table 2, Figure 2A*). Finally, the ceRNA network of GC included 62 DElncRNAs, 21 DEmiRNAs and 59 DE mRNAs (*Figure 2B*).

PPI network of GC patients

PPIs among the DE mRNAs identified from the ceRNA network were analyzed using the STRING website (*Figure 3A*). The bar plot figure revealed that the significant hub-genes were CHEK1, CDC25A, PBK, CEP55, and

E2F1 (*Figure 3B*).

GO and KEGG enrichment analyses

GO enrichment analysis was performed to explore the functions related to the DE mRNAs involved in the ceRNA network. *Figure 3C* displays the dot plot of GO terms. The top 3 GO terms of DE mRNAs in the ceRNA network were mainly enriched in DNA-binding transcription activator activity, proximal promoter sequence-specific DNA binding, and transcription coregulator activity. The KEGG pathways of the DE mRNAs were enriched in terms of cellular senescence and PI3K-Akt signaling pathway (*Figure 3D*).

Association between the ceRNA network and GC survival

The associations between the DElncRNAs, DEmiRNAs, and DE mRNAs and OS in GC patients were evaluated using the “survival” package in R software, in order to elucidate their prognostic characteristics. The results demonstrated that 9 out of 62 DElncRNAs, 5 out of 21 DEmiRNAs and 20 out of 59 DE mRNAs were significantly associated ($P < 0.05$) with OS in GC patients (*Figure 4*).

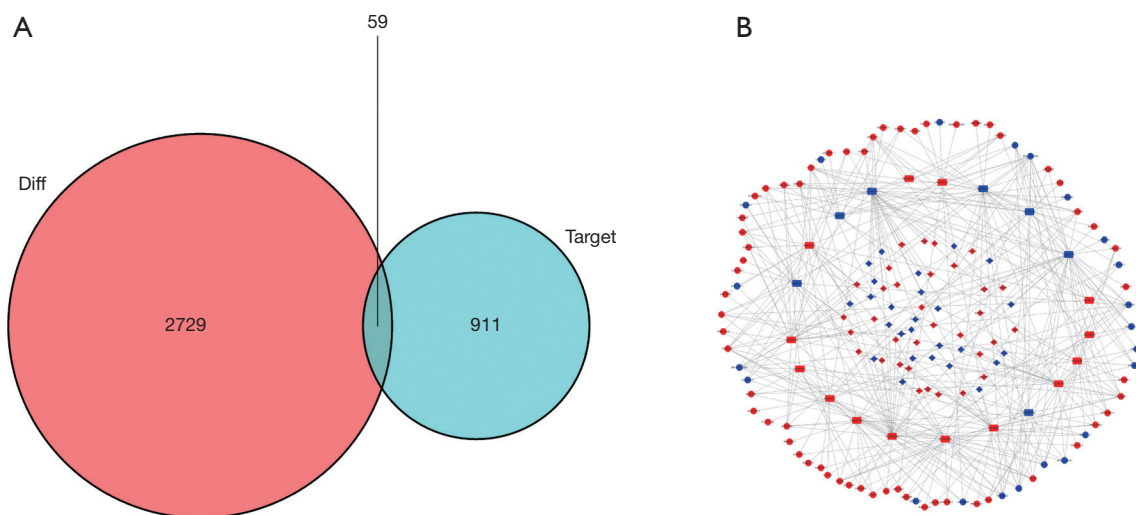


Figure 2 Establishment of the ceRNA network. (A) Venn diagram of the aberrantly expressed mRNAs related to ceRNA regulatory network. The red area indicates the total number of DEmRNA, while the blue area represents the target number. The intermediate purple area indicates the total number of the differentially expressed and targeted mRNAs. (B) The ceRNA network of GC patients. The red and blue nodes indicate upregulated and downregulated expression, respectively. lncRNA, miRNA and mRNA are shown as circles, rectangles, and diamonds, respectively. ceRNA, competing endogenous RNA; DEmRNA, differentially expressed mRNA; GC, gastric cancer.

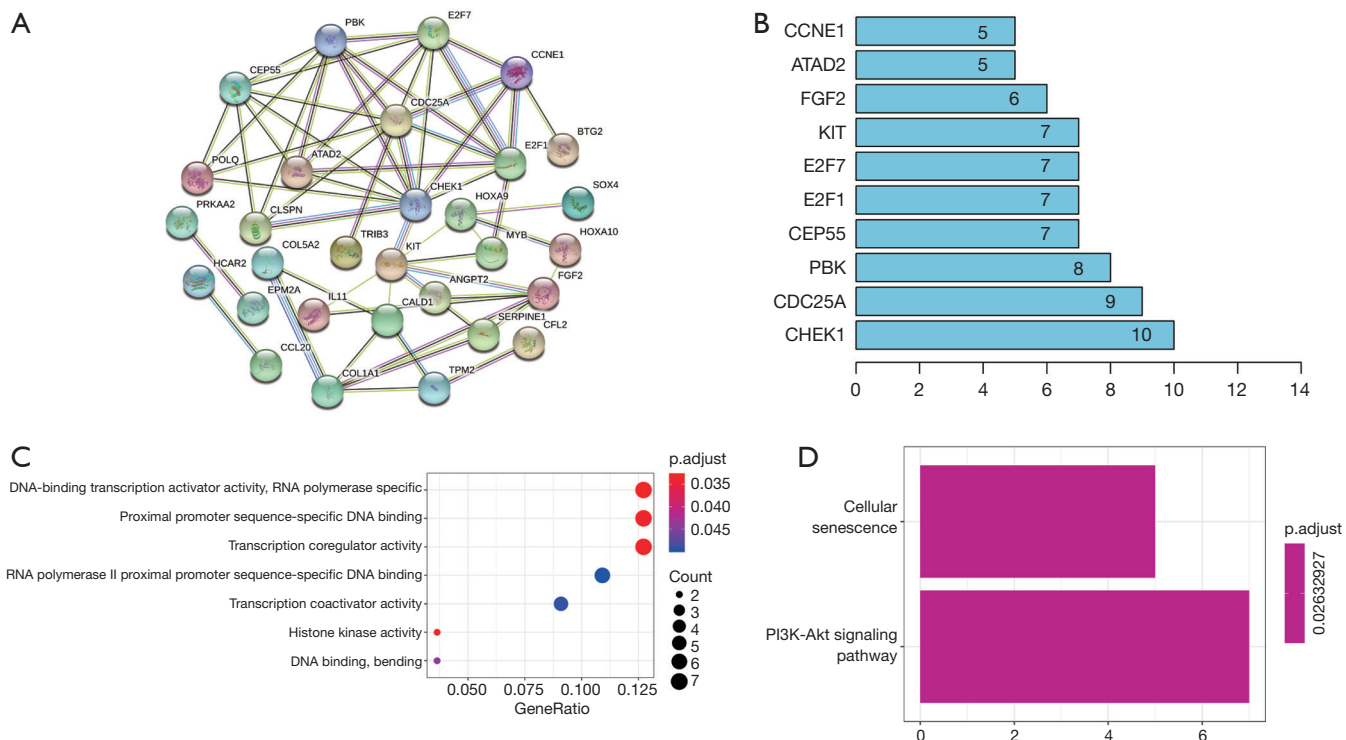


Figure 3 Construction of the PPI network and functional analyses. (A) PPI network analysis of mRNAs related to ceRNA regulatory network. (B) Barplot showing the degree of involvement of each gene in the PPI network. (C) GO analysis of DEmRNAs in the ceRNA network. (D) KEGG analysis of DEmRNAs in the ceRNA network. PPI, Protein-protein interaction; ceRNA, competing endogenous RNA; GO, Gene Ontology; KEGG, Kyoto Encyclopedia of Genes and Genomes.

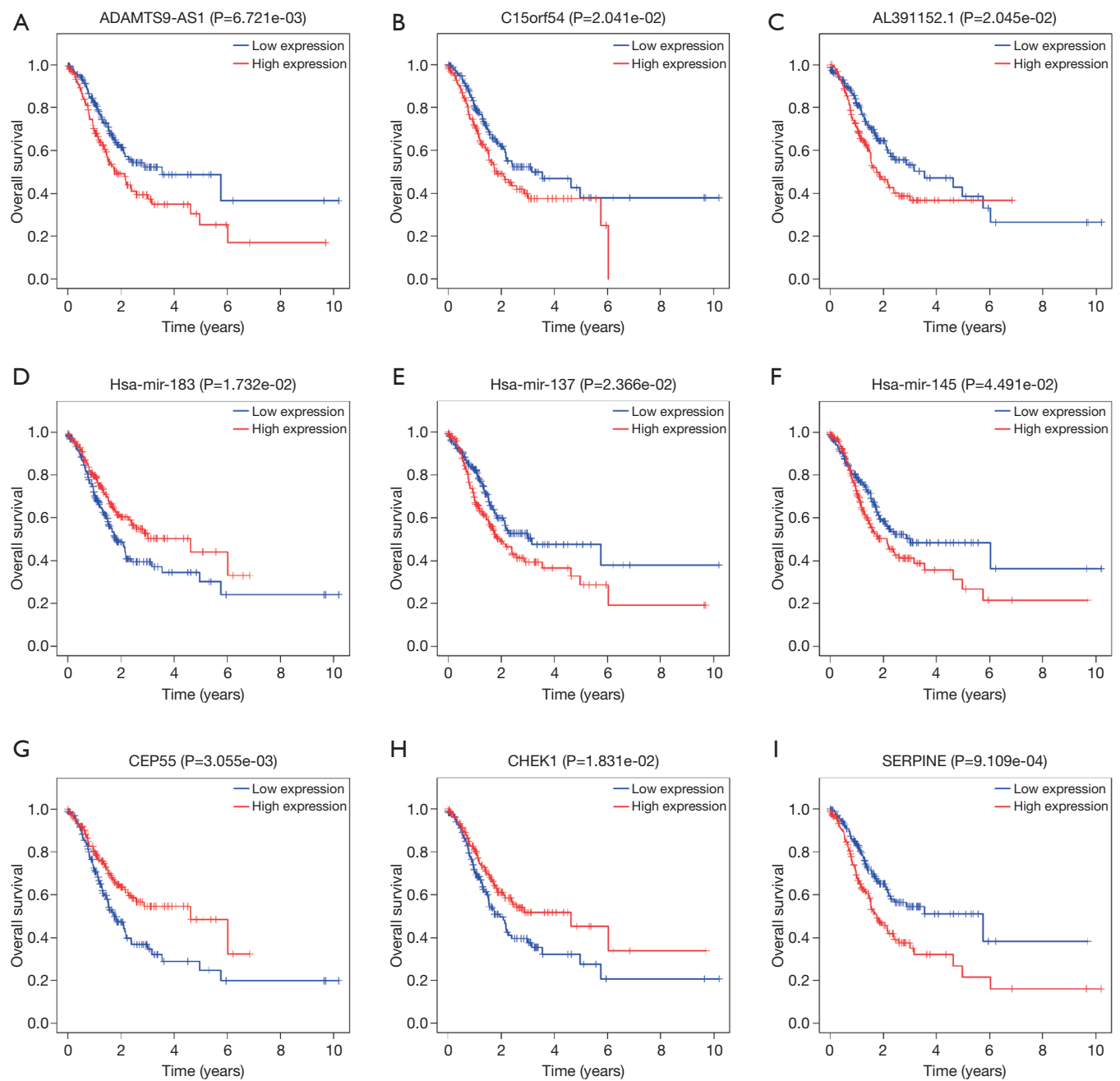


Figure 4 Associations of representative DElncRNAs (A,B,C), DEMiRNAs (D,E,F) and DEMRNAs (G,H,I) with over survival in GC patients. DElncRNAs, differentially expressed lncRNAs; DEMiRNAs, differentially expressed miRNAs; DEMRNAs, differentially expressed mRNAs; GC, gastric cancer.

lncRNA-based risk-scoring system for predicting GC prognosis

The results of univariate Cox regression analysis revealed that 4 lncRNAs were significantly associated with GC

prognosis ($P < 0.001$). Of these, 3 lncRNAs (i.e., ADAMTS9-AS1, C15orf54, and AL391152.1) remained significant in multivariate Cox regression analysis, and were thus selected for the construction of the risk-scoring system. The system consisted of the following equation: risk score = (0.195259

Table 3 Three lncRNAs correlated with overall survival in the predictive model

lncRNA	β	Hazard ratio	z	Pr(> z)
ADAMTS9-AS1	0.195259	1.215626	3.251301	0.001149
C15orf54	0.186247	1.20472	3.033521	0.002417
AL391152.1	0.183688	1.201641	3.672674	0.00024

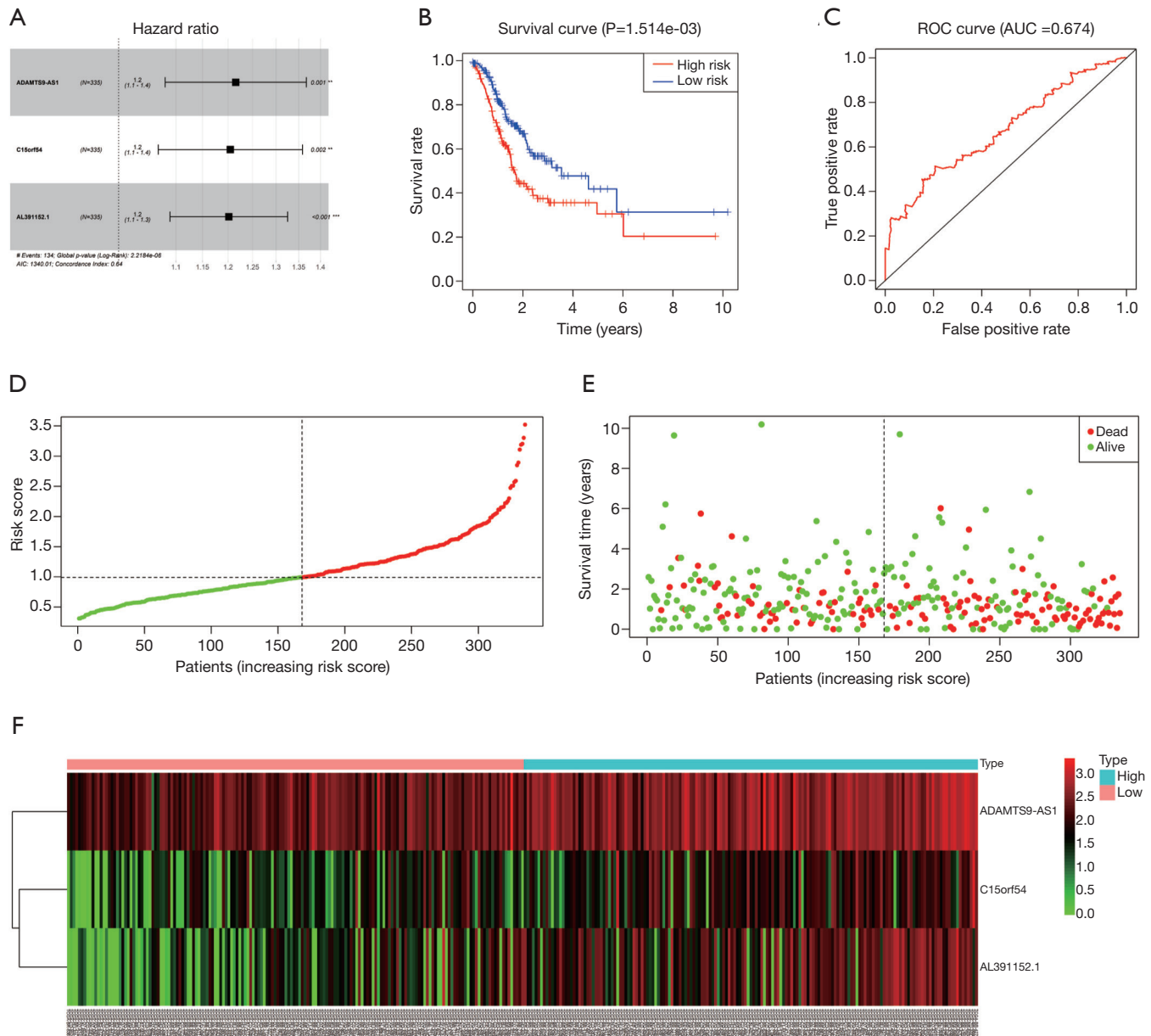


Figure 5 Risk scores of ADAMTS9-AS1, C15orf54, and AL391152.1 lncRNA-based prediction model. (A) Hazard ratio of the 3 lncRNAs involved in the risk-scoring system. (B) Kaplan-Meier curves for the prognosis of GC patients based on the 3 lncRNA signatures. (C) ROC curve of the 3 lncRNA-based prognostic signatures. (D) Distribution of risk score for each patient. (E) The risk score status of each patient. (F) Heat map of the 3 lncRNA-based prognostic signatures. ROC, receiver operating characteristic.

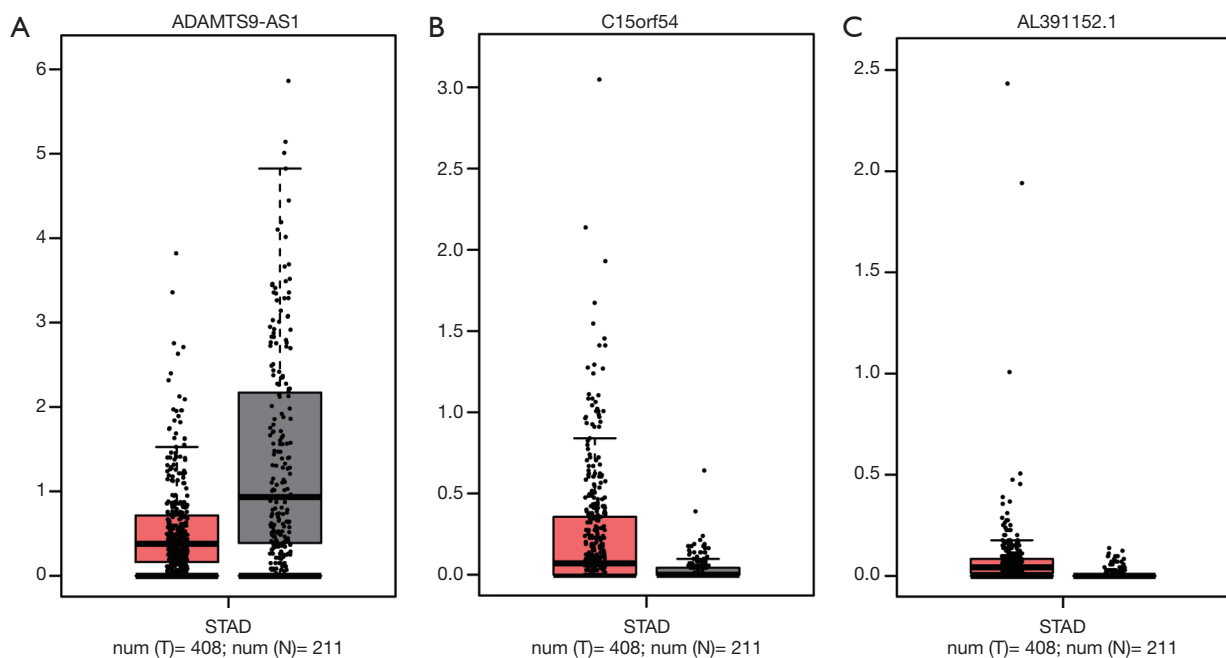


Figure 6 Validation of the expression of ADAMTS9-AS1 (A), C15orf54 (B), and AL391152.1 (C) in Gene Expression Profiling Interactive Analysis database. STAD, stomach adenocarcinoma.

\times ADAMTS9-AS1 expression) + (0.186247 \times C15orf54 expression) + (0.183688 \times AL391152.1 expression). As shown in *Table 3* and *Figure 5A*, the HR of ADAMTS9-AS1, C15orf54, and AL391152.1 was 1.2.

In order to explore the associations between prognostic lncRNAs and OS, survival curves were drawn using the Kaplan-Meier method (*Figure 5B*). The high-risk and low-risk groups consisted of 167 and 168 GC patients, respectively. The patients in the high-risk group exhibited significant shorter OS than those in the low-risk group ($P=1.514e-03$). The results indicate that the prognostic risk-scoring system based on these 3 lncRNAs were significantly related to OS.

Additionally, ROC curve analyses were implemented to assess the sensitivity and specificity of the risk-scoring system for predicting GC survival. The AUC value was calculated to be 0.674, with a concordance index (C-index) of 0.64 (95% CI: 0.59–0.69, $P=2.806485e-08$) (*Figure 5C*), suggesting that this risk-scoring system can effectively predict the prognosis of GC patients.

To demonstrate the distribution characteristics of the risk-scoring system, a heatmap plotting all of the individual risk scores was drawn (*Figure 5D*). The scatter plot and interactive distribution-based scatter plot for assessing the performance of the prognostic model are shown in

Figure 5E,F, respectively.

Furthermore, the expression of these 3 lncRNAs involved in the prognostic system were validated in GEPIA (*Figure 6*). The expression of ADAMTS9-AS1 was down-regulated in GC samples compared to normal tissues, while the expression of C15orf54 and AL391152.1 were up-regulated in GC samples, which were in concordance with our previous results. However, neither of these 3 lncRNAs expression levels were of statistical significance.

Association between the prognostic system and clinical characteristics

To further evaluate the clinical value of the prognostic system, correlations between the system and clinicopathological characteristics were analyzed. Our results shown that this prognostic system is positively associated with advanced tumor grade. Additionally, C15orf54 is also positively associated with high tumor grade (*Figure 7*).

The risk-scoring system based on 3 lncRNAs is an independent prognostic marker of GC

To clarify whether the prognostic ability of the risk-scoring system based on the 3 lncRNAs for survival prediction

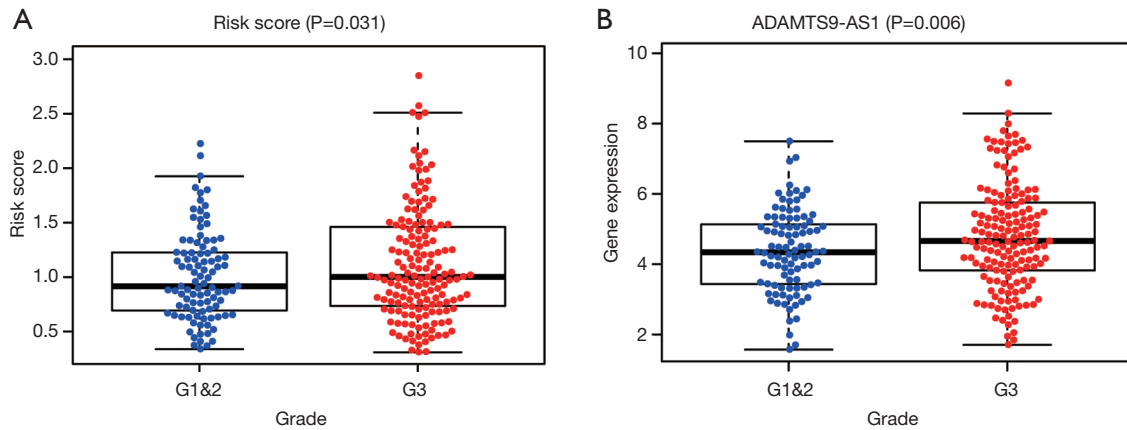


Figure 7 Association of the risk-scoring system with clinical characteristics. The risk-scoring system (A) and ADAMTS9-AS1 (B) were positively associated with advanced tumor grade.

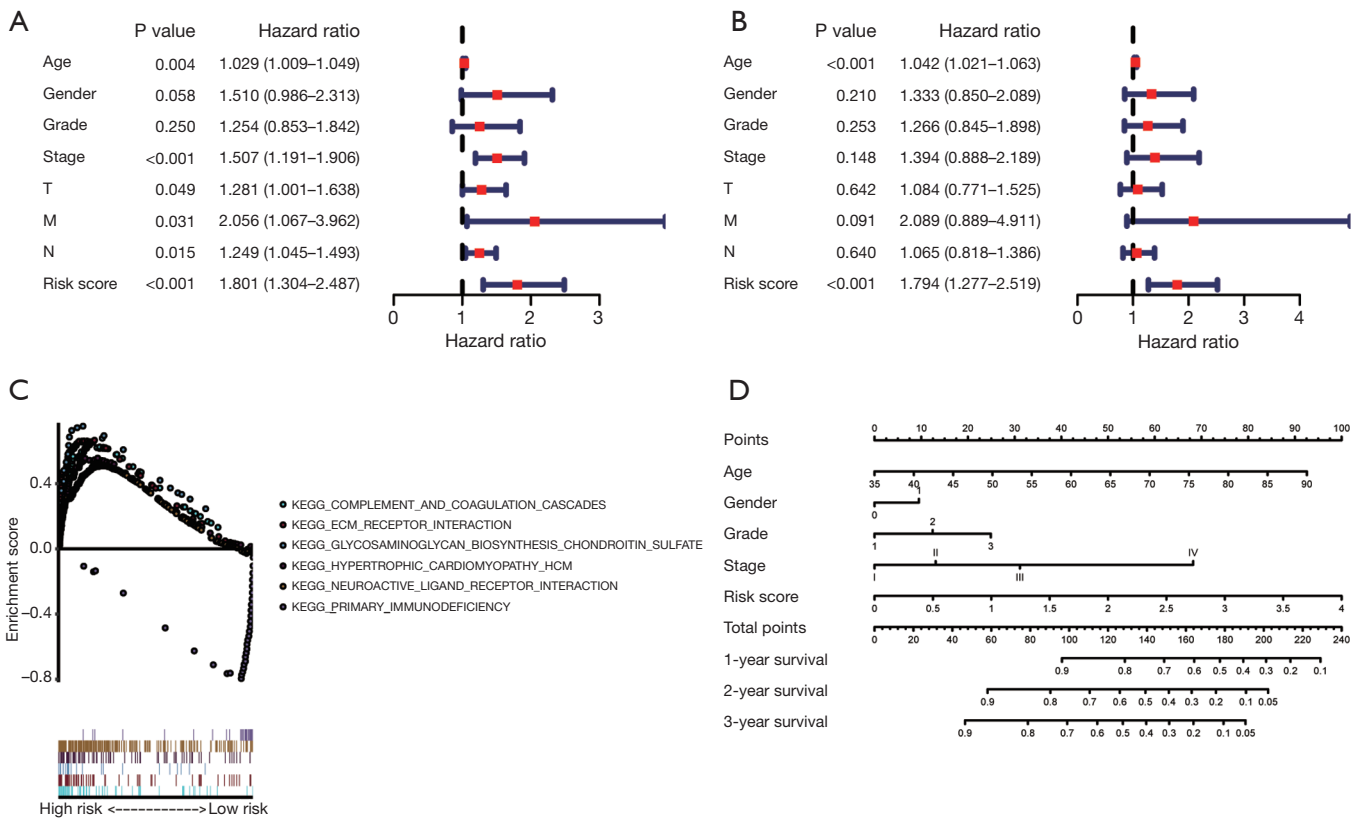


Figure 8 Univariate (A) and multivariable (B) Cox regression analyses for independence assessment of the 3-lncRNAs based risk-scoring system. (C) Gene set enrichment Analyses (GSEA) for comparing enriched KEGG pathways between the high risk group and the low risk group. (D) Prognostic nomogram for overall survival in patients with GC. KEGG, Kyoto Encyclopedia of Genes and Genomes; GC, gastric cancer.

was independent of other clinical features, univariate and multivariate Cox regression analysis of the system with other clinical features (age, gender, pathological grade, stage, and T, N, M stage) were performed. In the univariate Cox regression analysis (Figure 8A), the risk score (HR =1.801, 95% CI: 1.034–2.478, P<0.01), together with age (HR =1.029, 95% CI: 1.009–1.049, P=0.04) and stage (HR =1.507, 95% CI: 1.191–1.906, P<0.001), were significantly associated with the OS of patients with GC. However, in the multivariate Cox regression (Figure 8B), only the risk score (HR =1.794, 95% CI: 1.277–2.519, P<0.001) and age (HR =1.042, 95% CI: 1.021–1.063, P<0.001) were significantly associated with the OS of patients with GC. These results demonstrate that the risk-scoring system based on the 3 lncRNAs was an independent prognostic factor for GC.

GSEA

GSEA were performed and 5 gene sets were enriched in the high risk group with statically significance, while only 1 gene set was enriched in the low risk group with statically significance (Figure 8C). The pathways enriched in the high risk group were: “KEGG_NEUROACTIVE_LIGAND_RECEPTOR_INTERACTION”, “KEGG_ECM_RECEPTOR_INTERACTION”, “KEGG_GLYCOSAMINOGLYCAN_BIOSYNTHESIS_CHONDROITIN_SULFATE”, “KEGG_COMPLEMENT_AND_COAGULATION_CASCADES”, and “KEGG_HYPERTROPHIC_CARDIOMYOPATHY_HCM”. The pathway enriched in the low risk group was “KEGG_PRIMARY_IMMUNODEFICIENCY”.

Establishment of nomograms predicting prognosis in GC patients

Based on the results of independent risk factors on multivariate Cox regression analysis, a nomogram for the risk-scoring system (Figure 8D) combined with clinical features, including age, gender, pathological grade, and the stage, was established to visualize and predict GC patients' survival rate probability. The performance of the model was measured by the C-index comparing the predicted OS. Each factor was assigned points according to its risk to survival. For example, if a 60-year-old (41 points) female patient (0 points), with grade 2 (11 points), stage II (12 points) disease, and a high-risk score (98 points), had a total of 162 points, then, her 1-year, 2-year, and 3-year survival

would be about 60%, 28%, and 18%, respectively.

Discussion

Despite improvements in survival, the morbidity and mortality rates of GC remains high (1,6). Thus, the establishment of potential biomarkers and therapeutic targets as well as individualized approaches for treatment are urgently required. In the present work, a ceRNA network involving 62 DElncRNAs, 21 DEmiRNAs and 59 DEMRNAs, was constructed, in order to identify potential therapeutic targets and prognostic biomarkers for GC patients. In addition, 3 identified lncRNAs (i.e., ADAMTS9-AS1, C15orf54, and AL391152.1) were selected to construct a prognostic risk-scoring system for predicting the OS of GC patients. The AUC was considered good (0.674), along with a C-index of 0.64 (95% CI: 0.59–0.69, P=2.806485e-08). The scatter plot and interactive distribution-based scatter plot further demonstrated the high accuracy of the risk-scoring system. Both univariate and multivariate Cox regression independent analysis validated the predictive capability of the system. Furthermore, this risk-scoring system was positively associated with tumor grade. The expression of these 3 lncRNA were validated in GEPIA database. Our findings indicate that the risk-scoring system based on the 3 lncRNAs exhibited a robust ability to predict the prognosis of GC patients.

GSEA analyses results demonstrated that 5 gene sets are enriched in the high risk group with statically significance. Among them, neuroactive ligand receptor interaction pathway (24,25), ECM receptor interaction pathway (26), glycosaminoglycan biosynthesis chondroitin sulfate pathway (27) and complement and coagulation cascades pathway (28) were thought to be involved in tumorigenesis and progression, which further confirmed our results.

lncRNAs are known to play crucial roles in tumorigenesis and progression (7-9). Recently, some lncRNAs and lncRNA signatures have been identified as potential prognostic markers for GC. For example, Ma and colleagues reported a prognostic signature of 6-lncRNA in patients with GC based on microarray analysis (29). Through univariate and multivariate Cox regression analyses, Cai and colleagues identified 9 lncRNAs that were eventually filtered to construct a prognostic model, with AUC =0.795 (30). Accurate prognosis is the basis for developing appropriate treatment strategies for patients with cancer, therefore, considering clinical application

values, the number of lncRNAs in the model should be as small as possible, with high prognostic evaluation value. The AUC values of the models proposed in the literature are higher than that proposed in our study; however, the number of lncRNAs involved in the present study is lower than in other studies, with AUC =0.674.

The hypothesis regarding ceRNA has allowed for a better understanding of the functions of lncRNAs (10). lncRNAs can bind and sequester miRNAs, and therefore control the expression of targeted genes (10,13-15). Previous studies also have constructed a ceRNA network and identified significant hub-genes for GC, and some of these studies have discovered potential biomarkers for GC (31-39). Among them, 5 studies have found and validated predictive RNA biomarkers in GC tissues (31-34). Liu *et al.* have reported that 3 lncRNAs (i.e., LINC00111, AP002478, and LINC00313) and 2 mRNAs (COL1A1 and MYB) can serve as prognostic biomarkers for patients with *Helicobacter. pylori* (+) (35). Zhang *et al.* have reported that 3 lncRNAs (i.e.,UCA1, HOTTIP, and HMGA1P4) may contribute to the development and prognosis of GC, based on an analysis of Geno Expression Omnibus and TCGA database (37). However, all the biomarkers were not validated via independence assessment. Compared to these studies (29,31-36,38,39), we not only constructed a ceRNA network and identified a novel lncRNA based prognostic biomarker, but also validated that this lncRNA-based risk-scoring system is independent of other clinical features via using univariate and multivariate Cox independence analyses. Additionally, this risk-scoring system was positively associated with tumor grade, suggesting a potential of utilizing the system in GC diagnosis. A nomogram based on these 3 lncRNAs combined with other clinical information was generated to further predict the prognosis of GC patients, which can be convenient for clinical use.

However, there were some limitations in our research. First, the expression and function of these 3 lncRNAs should be validated in tissue or cell experiments. Second, this 3-lncRNA based risk-scoring system must be validated in large-scale clinical GC specimens. Finally, whether this 3-lncRNA based risk-scoring system combined with other clinical features can increase the predictive power, based on AUC values, remains an interesting question.

Conclusions

The ceRNA network that we constructed provide novel insights into the tumorigenesis of GC. The risk-

scoring system based on ADAMTS9-AS1, C15orf54 and AL391152.1 can be used to predict GC prognosis.

Acknowledgments

The authors would like to express their gratitude to Editage (<https://www.editage.cn/>) for the expert linguistics services provided.

Funding: This study was supported by the National Natural Science Foundation of China (81703916), Natural Science Foundation of Hunan Province (2018JJ6042), Hunan Provincial Health Department Project (B2015-78), Hunan Administration Traditional Chinese Medicine Foundation (201638), and Hunan Administration Traditional Chinese Medicine Foundation (201737).

Footnote

Peer Review File: Available at <http://dx.doi.org/10.21037/tcr-19-2977>

Conflicts of Interest: All authors have completed the ICMJE uniform disclosure form (available at <http://dx.doi.org/10.21037/tcr-19-2977>). The authors report grants from National Natural Science Foundation of China, grants from Hunan Provincial Natural Science Foundation, grants from Hunan Provincial Health Department Project, grants from Hunan Administration Traditional Chinese Medicine Foundation, during the conduct of the study.

Ethical Statement: The authors are accountable for all aspects of the work in ensuring that questions related to the accuracy or integrity of any part of the work are appropriately investigated and resolved. The present study was carried out in accordance with the TCGA guidelines (http://cancergenome.nih.gov/publications/publication_guidelines). Thus, it was not necessary to obtain further ethical approval.

Open Access Statement: This is an Open Access article distributed in accordance with the Creative Commons Attribution-NonCommercial-NoDerivs 4.0 International License (CC BY-NC-ND 4.0), which permits the non-commercial replication and distribution of the article with the strict proviso that no changes or edits are made and the original work is properly cited (including links to both the formal publication through the relevant DOI and the license). See: <https://creativecommons.org/licenses/by-nc-nd/4.0/>.

References

- Bray F, Ferlay J, Soerjomataram I, et al. Global cancer statistics 2018: GLOBOCAN estimates of incidence and mortality worldwide for 36 cancers in 185 countries. *CA Cancer J Clin* 2018;68:394-424.
- Biagioni A, Skalamera I, Peri S, et al. Update on gastric cancer treatments and gene therapies. *Cancer Metastasis Rev* 2019;38:537-48.
- Coutzac C, Pernot S, Chaput N, et al. Immunotherapy in advanced gastric cancer, is it the future? *Crit Rev Oncol Hematol* 2019;133:25-32.
- Puhr HC, Preusser M, Prager G, et al. New Treatment Options for Advanced Gastroesophageal Tumours: Mature for the Current Practice? *Cancers (Basel)* 2020;12.
- Matsuoka T, Yashiro M. Biomarkers of gastric cancer: Current topics and future perspective. *World J Gastroenterol* 2018;24:2818-32.
- Lordick F, Smyth EC. Two steps forward and one step back. *Nat Rev Clin Oncol* 2019;16:69-70.
- Li Y, Egranov SD, Yang L, et al. Molecular mechanisms of long noncoding RNAs-mediated cancer metastasis. *Genes Chromosomes Cancer* 2019;58:200-7.
- Ramnarine VR, Kobelev M, Gibb EA, et al. The evolution of long noncoding RNA acceptance in prostate cancer initiation and progression, and its clinical utility in disease management. *Eur Urol* 2019;76:546-59.
- Lim LJ, Wong SYS, Huang F, et al. Roles and Regulation of Long Noncoding RNAs in Hepatocellular Carcinoma. *Cancer Res* 2019;79:5131-9.
- Salmena L, Poliseno L, Tay Y, et al. A ceRNA hypothesis: the Rosetta Stone of a hidden RNA language? *Cell* 2011;146:353-8.
- Abdollahzadeh R, Daraei A, Mansoori Y, et al. Competing endogenous RNA (ceRNA) cross talk and language in ceRNA regulatory networks: A new look at hallmarks of breast cancer. *J Cell Physiol* 2019;234:10080-100.
- Klec C, Prinz F, Pichler M. Involvement of the long noncoding RNA NEAT1 in carcinogenesis. *Mol Oncol* 2019;13:46-60.
- Xiao G, Yao J, Kong D, et al. The Long Noncoding RNA TTTY15, Which Is Located on the Y Chromosome, Promotes Prostate Cancer Progression by Sponging let-7. *Eur Urol* 2019;76:315-26.
- Yang C, Shen S, Zheng X, et al. Long noncoding RNA HAGLR acts as a microRNA-143-5p sponge to regulate epithelial-mesenchymal transition and metastatic potential in esophageal cancer by regulating LAMP3. *FASEB J* 2019;33:10490-504.
- Zheng ZQ, Li ZX, Zhou GQ, et al. Long Noncoding RNA FAM225A Promotes Nasopharyngeal Carcinoma Tumorigenesis and Metastasis by Acting as ceRNA to Sponge miR-590-3p/miR-1275 and Upregulate ITGB3. *Cancer Res* 2019;79:4612-26.
- Tomczak K, Czerwinska P, Wiznerowicz M. The Cancer Genome Atlas (TCGA): an immeasurable source of knowledge. *Contemp Oncol (Pozn)* 2015;19:A68-77.
- Jeggari A, Marks DS, Larsson E. miRcode: a map of putative microRNA target sites in the long non-coding transcriptome. *Bioinformatics* 2012;28:2062-3.
- Li JH, Liu S, Zhou H, et al. starBase v2.0: decoding miRNA-ceRNA, miRNA-ncRNA and protein-RNA interaction networks from large-scale CLIP-Seq data. *Nucleic Acids Res* 2014;42:D92-7.
- Chou CH, Chang NW, Shrestha S, et al. miRTarBase 2016: updates to the experimentally validated miRNA-target interactions database. *Nucleic Acids Res* 2016;44:D239-47.
- Wong N, Wang X. miRDB: an online resource for microRNA target prediction and functional annotations. *Nucleic Acids Res* 2015;43:D146-52.
- Agarwal V, Bell GW, Nam JW, et al. Predicting effective microRNA target sites in mammalian mRNAs. *Elife* 2015;4.
- Otasek D, Morris JH, Boucas J, et al. Cytoscape Automation: empowering workflow-based network analysis. *Genome Biol* 2019;20:185.
- Tang Z, Kang B, Li C, et al. GEPIA2: an enhanced web server for large-scale expression profiling and interactive analysis. *Nucleic Acids Res* 2019;47:W556-60.
- Hong W, Yuan H, Gu Y, et al. Immune-related prognosis biomarkers associated with osteosarcoma microenvironment. *Cancer Cell Int* 2020;20:83.
- Shi K, Li N, Yang M, et al. Identification of Key Genes and Pathways in Female Lung Cancer Patients Who Never Smoked by a Bioinformatics Analysis. *J Cancer* 2019;10:51-60.
- Bao Y, Wang L, Shi L, et al. Transcriptome profiling revealed multiple genes and ECM-receptor interaction pathways that may be associated with breast cancer. *Cell Mol Biol Lett* 2019;24:38.
- Morla S. Glycosaminoglycans and Glycosaminoglycan Mimetics in Cancer and Inflammation. *Int J Mol Sci* 2019;20.
- Liu Y, Xiong S, Liu S, et al. Analysis of Gene Expression in Bladder Cancer: Possible Involvement of Mitosis

- and Complement and Coagulation Cascades Signaling Pathway. *J Comput Biol* 2020;27:987-98.
29. Ma B, Li Y, Ren Y. Identification of a 6-lncRNA prognostic signature based on microarray re-annotation in gastric cancer. *Cancer Med* 2020;9:335-49.
 30. Cai C, Yang L, Tang Y, et al. Prediction of Overall Survival in Gastric Cancer Using a Nine-lncRNA. *DNA Cell Biol* 2019;38:1005-12.
 31. Li CY, Liang GY, Yao WZ, et al. Integrated analysis of long non-coding RNA competing interactions reveals the potential role in progression of human gastric cancer. *Int J Oncol* 2016;48:1965-76.
 32. Chu A, Liu J, Yuan Y, et al. Comprehensive Analysis of Aberrantly Expressed ceRNA network in gastric cancer with and without H.pylori infection. *J Cancer* 2019;10:853-63.
 33. Gu W, Ren JH, Zheng X, et al. Comprehensive analysis of expression profiles of long noncoding RNAs with associated ceRNA network involved in gastric cancer progression. *Mol Med Rep* 2019;20:2209-18.
 34. Liu H, Zhang Z, Wu N, et al. Integrative Analysis of Dysregulated lncRNA-Associated ceRNA Network Reveals Functional lncRNAs in Gastric Cancer. *Genes (Basel)* 2018;9.
 35. Liu Y, Zhu J, Ma X, et al. ceRNA network construction and comparison of gastric cancer with or without *Helicobacter pylori* infection. *J Cell Physiol* 2019;234:7128-40.
 36. Yang J, Song H. Identification of long noncoding RNA RP11-169F17.1 and RP11-669N7.2 as novel prognostic biomarkers of stomach adenocarcinoma based on integrated bioinformatics analysis. *Epigenomics* 2019;11:1307-21.
 37. Zhang X, Zhang W, Jiang Y, et al. Identification of functional lncRNAs in gastric cancer by integrative analysis of GEO and TCGA data. *J Cell Biochem* 2019;120:17898-911.
 38. Peng S, Yin X, Zhang Y, et al. Competing endogenous RNA network analysis reveals potential long non-coding RNAs as predictive biomarkers of gastric cancer. *Oncol Lett* 2020;19:2185-96.
 39. Qi M, Yu B, Yu H, et al. Integrated analysis of a ceRNA network reveals potential prognostic lncRNAs in gastric cancer. *Cancer Med* 2020;9:1798-817.

Cite this article as: Liu M, Li J, Huang Z, Li Y. Gastric cancer risk-scoring system based on analysis of a competing endogenous RNA network. *Transl Cancer Res* 2020;9(6):3889-3902. doi: 10.21037/tcr-19-2977